Cancer Letters ■■ (2016) ■■–■■

Contents lists available at ScienceDirect

Cancer Letters

journal homepage: www.elsevier.com/locate/canlet

Original Articles

Metabolic alterations and drug sensitivity of tyrosine kinase inhibitor resistant leukemia cells with a FLT3/ITD mutation

Amin Huang [a,b,1], Huaiqiang Ju [a,1], Kaiyan Liu [a,1], Guilian Zhan [a], Daolu Liu [a], Shijun Wen [a], Guillermo Garcia-Manero [c], Peng Huang [a,b,*], Yumin Hu [a,*]

[a] Sun Yat-sen University Cancer Center, State Key Laboratory of Oncology in South China, Collaborative Innovation Center for Cancer Medicine, Guangzhou, China
[b] Department of Translational Molecular Pathology, The University of Texas M.D. Anderson Cancer Center, Houston, TX, USA
[c] Department of Leukemia, The University of Texas M.D. Anderson Cancer Center, Houston, TX, USA

ARTICLE INFO

Article history:
Received 15 February 2016
Received in revised form 24 April 2016
Accepted 25 April 2016

Keywords:
FLT3/ITD
TKI resistance
Mitochondria
Metabolic alterations
Glycolysis

ABSTRACT

Internal tandem duplication (ITD) of the juxtamembrane region of FMS-like tyrosine kinase-3 (FLT3) receptor is a common type of mutation in adult acute myeloid leukemia (AML), and patient response to FLT3 inhibitors appears to be transient due to the emergence of drug resistance. We established two sorafenib-resistant cell lines carrying FLT3/ITD mutations, including the murine BaF3/ITD-R and human MV4-11-R cell lines. Gene expression profile analysis of the resistant and parental cells suggests that the highest ranked molecular and cellular functions of the differentially expressed genes are related to mitochondrial dysfunction. Both murine and human resistant cell lines display a longer doubling time, along with a significant inhibition of mitochondrial respiratory chain activity and substantial upregulation of glycolysis. The sorafenib-resistant cells exhibit increased expression of a majority of glycolytic enzymes, including hexokinase 2, which is also highly expressed in the mitochondrial fraction and is associated with resistance to apoptotic cell death. The sorafenib-resistant cells are collaterally sensitive to a number of glycolytic inhibitors including 2-deoxyglucose and 3-bromopyruvate propylester. Our study reveals a metabolic signature of sorafenib-resistant cells and suggests that glycolytic inhibition may override such resistance and warrant further clinical investigation.

Introduction

FMS-like tyrosine kinase 3 (FLT3) plays a critical role in regulation of normal hematopoiesis. Internal tandem duplication (ITD) in the juxtamembrane region of FLT3 is observed in a substantial proportion of AML patients and predicts poor prognosis [1,2]. ITD mutation in the FLT3 receptor gene leads to constitutive activation of downstream pathways such as MEK/ERK, PI3K/AKT, and JAK/STAT [3,4], which may contribute to leukemogenesis. A number of FLT3 inhibitors under clinical investigation have shown some biological activity, yet patient response tends to be transient, as the major challenge to FLT3-targeted therapy appears to be the emergence of resistance [4,5]. Sorafenib is a tyrosine kinase inhibitor of FLT3, VEGFR, PDGFR, and Raf and has shown initial anti-leukemia effects in patients with relapsed or refractory FLT3/ITD AML [6].

The acquisition of secondary mutations in the FLT3 kinase domain has been recognized as one of the primary causes of resistance to FLT3 inhibitors [7–9]. Non-mutational mechanisms such as activation of pro-survival pathways, including MEK/ERK, PI3K/AKT, JAK/STAT, and NF-κB, have also been reported [4,10–12]. Although certain key molecules and signaling pathways have been identified, the metabolic changes to FLT3 inhibitor-resistant cells and the relevance of metabolic changes to drug resistance remain to be investigated. Prominent features of cancer cells include metabolic reprogramming and enhanced resistance to mitochondrial apoptosis. The reliance of cancer cells on glycolysis to meet metabolic demands has been termed the Warburg effect and is an emerging hallmark of cancer [13].

In the current study, murine (BaF3/ITD-R) and human (MV4-11-R) sorafenib-resistant cell lines carrying FLT3/ITD mutations were established by increasing exposure to sorafenib. Both BaF3/ITD-R and MV4-11-R cells showed varying degrees of cross-resistance to other FLT3 inhibitors. mRNA microarray analysis of MV4-11-R cells revealed that mitochondrial dysfunction was the highest-ranked gene set with significant change when compared to the parental MV4-11 cells. Because the mitochondrial respiratory chain is the major site for ATP generation, when mitochondrial oxidative phosphorylation is compromised, cells are able to adapt by using alternative metabolic pathways, such as glycolysis, to maintain the energy supply. From a therapeutic standpoint, it is important to test the

* Corresponding authors. Tel.: +86 20 87343171; fax: +86 20 87335190.
E-mail addresses: huangpeng@sysucc.org.cn (P. Huang); huym@sysucc.org.cn (Y. Hu).
[1] These authors contributed equally to this work.

http://dx.doi.org/10.1016/j.canlet.2016.04.040
0304-3835/

dependence of sorafenib-resistant cells on glycolysis for ATP generation and develop new strategies that overcome resistance to FLT3 tyrosine kinase inhibitors. Several agents, including 2-deoxyglucose (2-DG) and 3-bromopyruvate propylester (3-BrOP), have been shown to abolish ATP generation through the glycolytic pathway [14,15]. Our recent studies demonstrated that 3-BrOP is a potent inhibitor of both hexokinase 2 and GAPDH and effectively eradicates residual cancer stem cells that are resistant to chemotherapeutic agents [16–18].

In the current study, we aimed to evaluate the metabolic signature of sorafenib-resistant cells, characterize the role of glycolytic enzymes in association with resistance to sorafenib-induced cell death and examine the therapeutic effects of glycolytic inhibitors in resistant cells. Our study provides a greater understanding of alternative mechanisms of resistance to tyrosine kinase inhibitors in the context of metabolic alterations and potential therapeutic strategies in the treatment of FLT3/ITD leukemia.

Materials and methods

Cell lines and cell culture

The mouse hematopoietic progenitor cell line BaF3 was stably transfected with FLT3/ITD (BaF3/ITD), as previously described [19], and was kindly provided by Dr. Donald Small (Johns Hopkins University, Baltimore, MD). The human AML-derived MV4-11 cell line expressing the FLT3/ITD mutation was obtained from the ATCC. BaF3/ITD and MV4-11 cell lines were cultured in RPMI 1640 medium with 10% FBS. BaF3/ITD-R and MV4-11-R cells were established by culturing in increasing concentrations of sorafenib, with initial concentration of 1 nM, until both cell lines survived a concentration of 500 nM. Both resistant cell lines were then maintained in complete RPMI 1640 medium containing 500 nM sorafenib.

Reagents and antibodies

Sorafenib tosylate and MLN518 were purchased from Selleck Chemicals. PKC412, 2-deoxy-D-glucose (2-DG) and sodium dichloroacetate (DCA) were purchased from Sigma-Aldrich. 3-BroP was synthesized as previously described [20]. The following antibodies were used for immunoblotting analysis: Mito Profile® Total OXPHOS Antibody Cocktail and rabbit anti-cytochrome C (Abcam); rabbit anti-HK2, anti-PKM2, anti-PDK-1, anti-P-FLT3, anti-FLT3, anti-Akt, anti-P-p44/42MAPK, anti-p44/42MAPK, anti-RPS6, anti-P-RPS6, anti-HSP60, and anti-Bax; mouse anti-P-Akt and anti-β-actin (Cell Signaling Technologies).

Cell proliferation and cytotoxicity assays

Cell proliferation was measured using MTS assay (CellTiter 96 AQueous One Solution, Promega), and apoptotic cell death was detected by annexin-V/PI staining, as previously described [21].

Quantitative real-time PCR

Quantitative real-time PCR was performed using SYBR® Premix Ex Taq™ II (Clontech) and CFX96 real-time PCR detection system (Bio-Rad). Human gene-specific primers were synthesized by Invitrogen, and sequences are shown in Supplementary Table S1.

Isolation of mitochondria

Mitochondria of MV4-11-R cells were isolated using Qproteome Mitochondria Isolation Kit (Qiagen). Briefly, cells were was washed and re-suspended in Disruption Buffer to remove nuclei, cell debris, and unbroken cells. The supernatant was centrifuged to collect crude mitochondria pellet. After removal of the supernatant, the mitochondria pellet was re-suspended in Mitochondria Purification Buffer. Finally, the mitochondria were re-suspended in lysis buffer containing 8 M urea, 4% CHAPS, 65 mM DTT, and 40 mM Tris and then were sonicated. The sample was finally centrifuged, and the supernatant, which contained mitochondrial protein lysates, was obtained.

Measurement of intracellular ATP levels

The level of intracellular ATP was measured by the CellTiter-Glo Luminescent Cell Viability Assay (Promega). One million cells/mL were seeded in triplicate in six-well plates and treated with indicated compounds. After normalization, 100 µL of cells was transferred to a 96-well plate and mixed with 100 µL of reagents. The mixture was incubated at room temperature for 10 min before the luminescence was detected by a SpectraMax microplate reader.

GAPDH activity detection

GAPDH activity was measured by the KDalert™ GAPDH Assay Kit (Invitrogen). 1×10^5 cells were collected and washed with PBS, and 100 µl of lysis buffer was added to each sample before incubation at 4 °C for 20 min. Additionally, 10 µL of sample lysate was transferred to a 96-well microplate and mixed with 90 µL of Master Mix. GAPDH activity signal was measured immediately with a fluorescence plate reader and recorded for 20 min.

Glucose uptake and lactate production

Cells in the exponential growth phase were seeded in triplicate at a density of 1×10^6 cells/well in six-well plates. Culture media were removed after a 6-h incubation for analysis of glucose and lactate levels by an SBA-40C Biosensor (Biology Institute of the Shandong Academy of Science, Jinan, Shandong Province, China). Glucose uptake or lactate production was determined by the concentration difference between cell culture medium and fresh medium without cells.

mRNA microarray and Ingenuity Pathway Analysis (IPA)

Baseline gene expression profiles of MV4-11 and MV4-11-R cells were analyzed by Agilent SurePrint G3 Human Gene Expression 8 × 60K Microarray (Agilent Technologies). Total RNA of both cell lines was prepared in triplicate. After DNA hybridization, the array was scanned using the ScanArray Express scanner (Packard Bioscience, Kanata, OT) and analyzed with GenePixro 4.0 (Axon Instruments, Foster City, CA). The data were then subjected to summarization, normalization and quality control using GeneSpring software V12 (Agilent Technologies). Threshold values of ≥2 and ≤–2-fold change and a Benjamini–Hochberg corrected p value of 0.05 were calculated to select the differentially expressed genes. The data were median centered by genes using the Adjust Data function of CLUSTER 3.0 and further analyzed by hierarchical clustering using average linkage. Finally, tree visualization was performed using Java Treeview (Stanford University School of Medicine, Stanford, CA). The data are available through NCBI Gene Expression Omnibus with an accession number GSE74666. Differentially expressed genes were investigated by Ingenuity Pathway Analysis (Ingenuity, Redwood City, CA) to identify the relevant biological functions that were most significant in the data sets. A fold change of ≥ or ≤2 and a p value < 0.05 were used as cut-off values.

Real time bioenergetics analysis

Cellular bioenergetics, including oxygen consumption rate and extracellular acidification rate, were measured by Seahorse Bioscience XF-24 Extracellular Flux Analyzer. A 24-well cell culture microplate was coated with Corning® Cell-Tak™ Cell and Tissue Adhesive (Corning Incorporated) to allow adhesion of suspended cells. After calibration of the analyzer, sequential compound injections, including oligomycin A, carbonyl-cyanide p-trifluoromethoxyphenylhydrazone (FCCP), antimycin A and rotenone, were applied on the microplate to test mitochondrial respiration. Sequential compound injections, including glucose, oligomycin A and 2-DG, were applied to test glycolytic activity. Oxygen consumption rate was also measured by a Clark-type oxygen electrode disc (Oxytherm, Hansatech Instrument, Cambridge, UK), as described previously [22].

Statistical analysis

The data were expressed as means ± SEM. The difference between two groups of data was evaluated by Student's paired t test or two-way ANOVA, and the difference between more than two groups was evaluated by one-way ANOVA (Prism GraphPad). A p value of less than 0.05 was considered statistically significant.

Results

BaF3/ITD-R and MV4-11/R are highly resistant to FLT3 inhibitors and exhibit upregulation of FLT3 downstream effectors

We first compared apoptotic cell death induced by sorafenib in the parental cell lines (BaF3/ITD, MV4-11) to the resistant cell lines (BaF3/ITD-R and MV4-11-R). Two pairs of cell lines were treated with varying concentrations of sorafenib for 48 h and subjected to annexin-V/PI staining (Fig. 1A). The results demonstrated that 1 and 3 µM sorafenib caused cell death in 68% and 35% of the population of BaF3/ITD and MV4-11 cells, respectively. However, the same concentrations of sorafenib did not affect apoptotic cell death in both resistant cell lines. Additionally, 10 µM sorafenib caused massive cell death (>90%) in BaF3/ITD and MV4-11 cells, yet only induced 33% and 14% cell death in BaF3/ITD-R and MV4-11-R cells, respectively. The cytotoxic effects of other FLT3 inhibitors, including PKC412

Please cite this article in press as: Amin Huang, et al., Metabolic alterations and drug sensitivity of tyrosine kinase inhibitor resistant leukemia cells with a FLT3/ITD mutation, Cancer Letters (2016), doi: 10.1016/j.canlet.2016.04.040

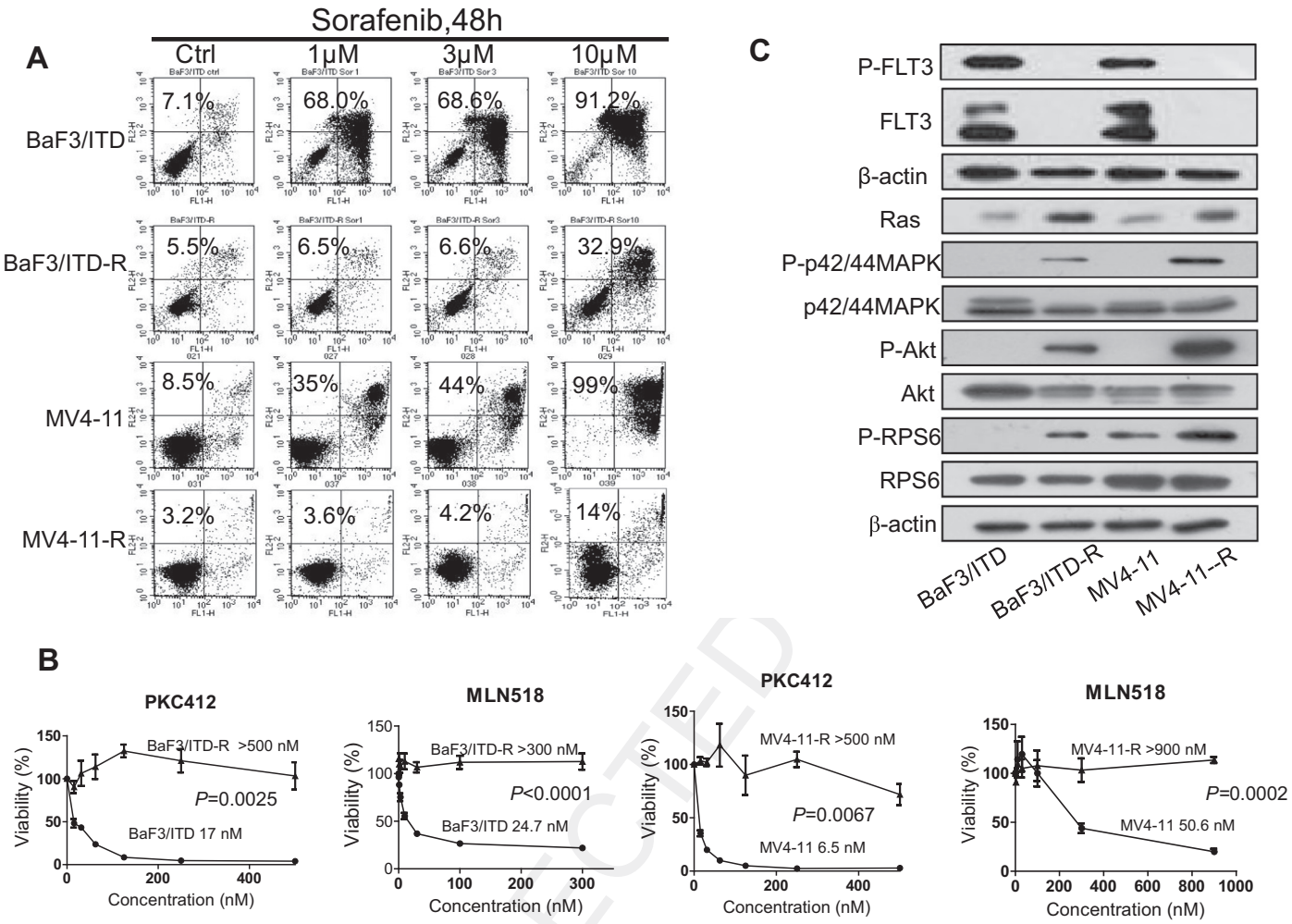

Fig. 1. Sorafenib-resistant cells show cross-resistance to different FLT3 tyrosine kinase inhibitors and upregulation of pro-survival pathways. (A) BaF3/ITD, BaF3/ITD-R, MV4-11 and MV4-11-R cells were treated with the indicated concentration of sorafenib for 48 h and subjected to annexin-V/PI assay. Percentage values indicate cell death populations. (B) BaF3/ITD, BaF3/ITD-R, MV4-11 and MV4-11-R cells were treated with various concentrations of type I (PKC412) and type II tyrosine kinase inhibitor (MLN518) for 72 h and subjected to MTS assay. Numbers above the curves indicate IC_{50} of these compounds in each cell line. The results were statistically significant as shown by p values. Error bars represent SEM. (C) Immunoblotting analysis of phosphorylated-FLT3 (p-FLT3), total FLT3, Ras, total p42/44MAPK, phosphorylated p42/44MAPK (p- p42/44MAPK), phosphorylated-Akt, total Akt, phosphorylated-RPS6 (p-RPS6), total RPS6 in BaF3, BaF3/ITD-R, MV4-11, MV4-11-R cells. β-actin was used as loading control.

and MLN518 [23,24], were also tested in the parental and resistant cell lines. The IC_{50} values of PKC412 (Midostaurin) and MLN518 (Tandutinib) were evaluated by a 72-h MTS assay. Both resistant cell lines exhibited substantially higher (>12- to 70-fold) IC_{50} values when treated with PKC412 or MLN518 than their parental cell lines (Fig. 1B). We also examined downstream effector pathways of FLT3 in both parental and resistant cell lines. Western blotting analysis in Fig. 1C showed lack of total FLT3 and phosphorylated-FLT3 expression in BaF3/ITD-R and MV4-11-R cells when compared to their parental cells. Both resistant cell lines showed a higher expression of proteins in the MAPK/RAS and PI3K/Akt signaling pathways, including Ras, phospho-MAPK, phospho-Akt and phospho-S6 ribosomal protein (RPS6). Our results demonstrated that although FLT3 remained inhibited, sorafenib-resistant cell lines exhibited continued activation of downstream effector pathways.

Gene set expression analysis of MV4-11 and MV4-11-R cell lines

To further analyze the effect of prolonged exposure to sorafenib on MV4-11 cells, we performed mRNA microarray analysis to identify candidate molecules involved in the cellular response. Ingenuity Pathway Analysis (IPA) revealed that the highest ranked molecular and cellular functions of the differentially expressed genes in these cell lines were closely associated with depolarization of mitochondria, mitochondrial dysfunction, G2/M cell cycle checkpoint and anti-apoptosis (Table 1).

Sorafenib-resistant cells exhibit a higher percentage of cells in the G2 phase of the cell cycle

To verify the results of gene set expression analysis, we compared the cell cycle phases and cell growth rates of the resistant and parental cells. Both BaF3/ITD-R (15.2%) and MV4-11-R (12.9%)

Table 1
Ingenuity analysis of top ranked pathways affected in differentially expressed genes between MV4-11 and MV4-11-R.

Pathways	Ratio[Δ]	p-value
Decreased depolarization of mitochondria and mitochondrial membrane	19/19	2.46E–02
Mitochondrial dysfunction	111/126	4.98E–02
Cell cycle:G2/M DNA damage checkpoint regulation	39/41	1.6E–02
Anti-apoptosis	29/31	6.91E–02

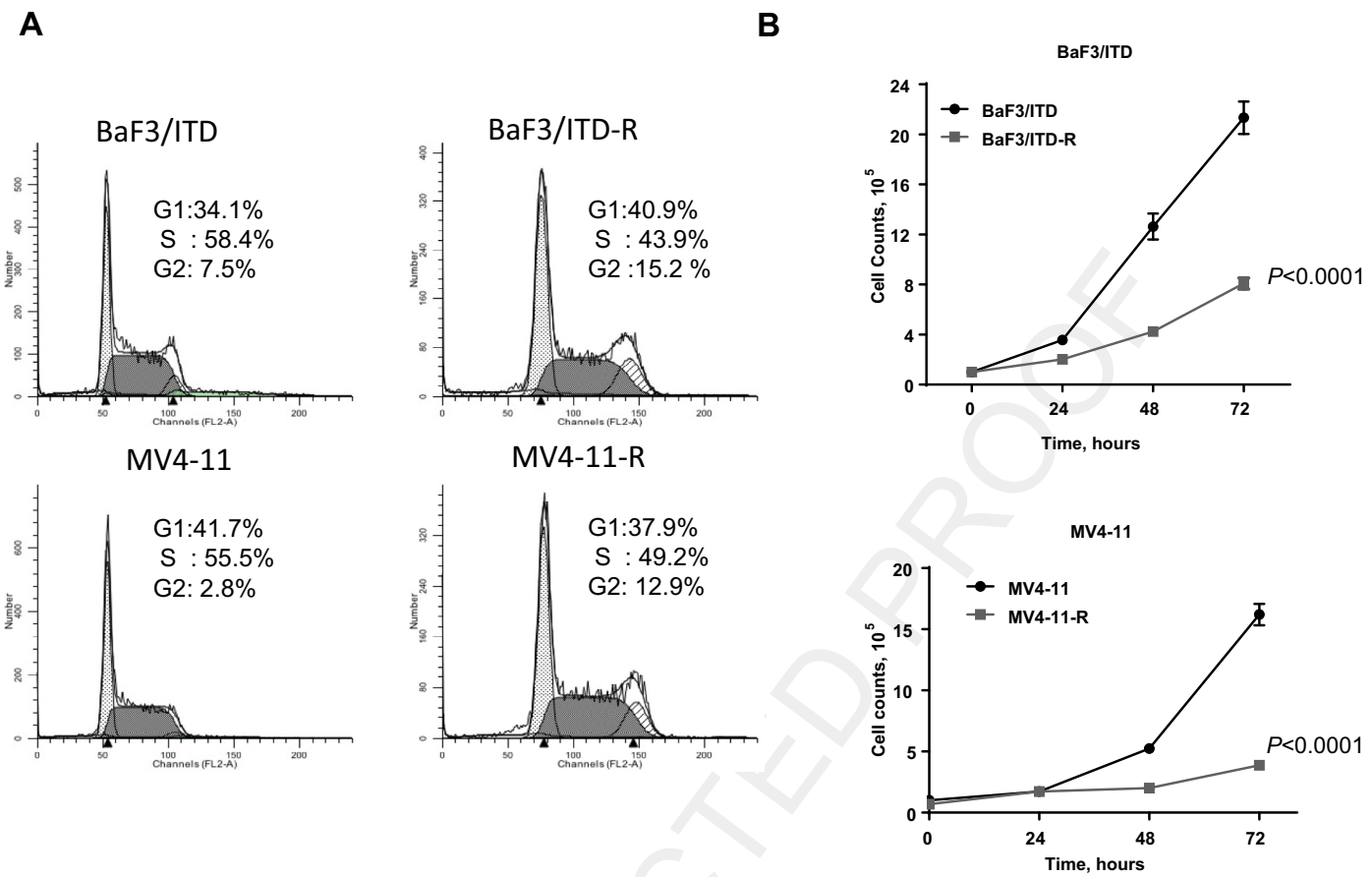

Fig. 2. G2 cell cycle arrest and cell growth curve of sorafenib-resistant cells. (A) Cell cycle analysis of BaF3/ITD, BaF3/ITD-R, MV4-11 and MV4-11-R cells. Numbers indicate the percentage of cells in different phases of cell cycle. (B) Equal numbers (1×10^5) of BaF3/ITD, BaF3/ITD-R, MV4-11 and MV4-11-R cells were started in cell culture and total cell numbers were counted every 24 h for up to 72 h using a Coulter Z_2 Particle Counter & Size analyzer. The results were statistically significant as shown by p values. Error bars represent SEM.

cells consistently showed a higher percentage of cells in the G2 phase than BaF3/ITD (7.5%) and MV4-11 (2.8%) cells (Fig. 2A). A 72 h long cell proliferation assay, which involved directly counting cells, indicated that both resistant cell lines exhibited a significant delay of cell growth when compared to the parental cells (Fig. 2B). Thus, our evaluation of cell cycles and proliferation appears to validate the results that the G2/M cell cycle checkpoint is a top-ranked pathway altered in the sorafenib-resistant cells.

Impaired mitochondrial bioenergetics in sorafenib-resistant cells

The gene set analysis of MV4-11-R versus MV4-11 cells by IPA also indicated decreased depolarization of mitochondria, and mitochondrial membrane, mitochondrial dysfunction and anti-apoptosis as a top-ranked molecular or cellular function identified by the differential gene sets (Table 1). It is known that the primary metabolic function of mitochondria is to carry out oxidative phosphorylation and generate the ATP required to support cellular functions; in addition, mitochondrial outer membrane permeabilization mediates the intrinsic pathway of apoptosis [25]. Real-time extracellular flux analysis by Seahorse XF24 was performed as previously described [26,27] to investigate the pathways identified by IPA. Oxygen consumption rate (OCR), which reflects mitochondrial respiration, was measured by exposing cells, by injection, to four well-defined small molecules sequentially. As shown in Fig. 3A, the curve of the first 20 min without injection represented basal OCR, and BaF3/ITD-R cells showed an approximately 50% decrease in OCR when compared to BaF3/ITD cells, reflecting attenuated mitochondrial respiration. The decrease in OCR upon injection of the ATP synthase inhibitor oligomycin (1 μM) represented the period during respiration where ATP is produced. The second injection of FCCP (2 μM) uncouples mitochondrial respiration by carrying protons across the inner membrane, thus stimulating oxygen consumption to maximum capacity [27]. The third injection consisted of a mitochondrial respiratory chain complex I inhibitor rotenone (1 μM) and complex III inhibitor antimycin A (1 μM) to shut down total electron flow. Fig. 3A showed that FCCP induced a rapid increase in OCR by BaF3/ITD cells and moderated response by BaF3/ITD-R, indicating impaired spare respiratory capacity in the sorafenib-resistant cells. This mitochondrial bioenergetic profile was also observed in MV4-11-R cells when compared to MV4-11 cells. Oxygen consumption rate was also assessed using an Oxytherm respiration chamber as previously described [28]. Fig. 3B demonstrated 42% (BaF3/ITD-R) and 58% (MV4-11-R) decrease in oxygen consumption rate in the sorafenib-resistant cells when compared to the parental cells.

To study the underlying mechanisms of decreased mitochondrial respiration in sorafenib-resistant cells, we examined the expression of the mitochondrial respiratory chain components using western blot analysis for the representative subunits of each mitochondrial electron transport complex (I, II, III, IV and V). Interestingly, we observed down-regulation of the complexes I-NDUFB8, II-SDHB and III-UQCRC2 and up-regulation of complexes IV-COXII and V-ATP5A in both resistant cell lines (Fig. 3C), which likely reflects an impaired electron flux along the respiratory chain and the compensatory effect of ATP synthase (complex

Please cite this article in press as: Amin Huang, et al., Metabolic alterations and drug sensitivity of tyrosine kinase inhibitor resistant leukemia cells with a FLT3/ITD mutation, Cancer Letters (2016), doi: 10.1016/j.canlet.2016.04.040

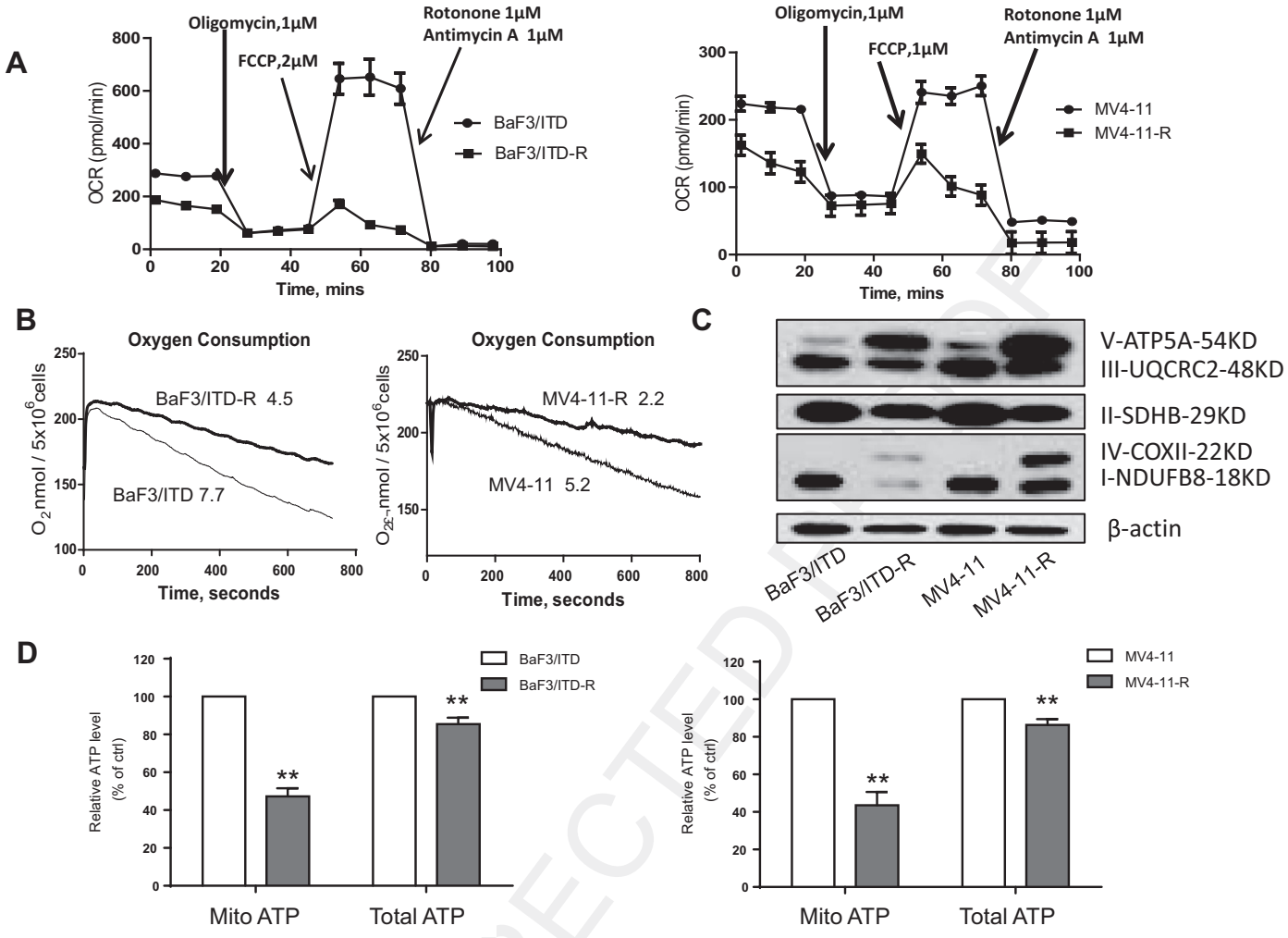

Fig. 3. Mitochondrial dysfunction in sorafenib-resistant cells. (A) Pharmacological profile of oxygen consumption rate (OCR) was monitored with a Seahorse XF24 analyzer for 100 min. The metabolic inhibitors oligomycin, FCCP, rotenone and antimycin were injected sequentially at different time points as indicated. Left panel: Murine cells BaF3/ITD and BaF3/ITD-R. Right panel: Human cells MV4-11 and MV4-11-R. (B) Comparison of mitochondrial respiration of the parental and sorafenib-resistant cells measured by a Clark-type oxygen electrode disc as described in the Materials and methods section. Numbers above the curves indicate oxygen consumption rate (nmol/min). (C) Immunoblotting analysis of mitochondrial respiratory chain complex I to V in the parental and sorafenib-resistant cells. β-actin was used as loading control. (D) Quantitative analysis of mitochondria-derived ATP and total ATP generation in the parental and sorafenib-resistant cells. Bars, means ± SEM. $^{**}p < 0.01$, n = 3.

V) to cope with the energy crisis caused by loss of function in electron carriers. Indeed, calculations obtained from extracellular flux analysis using Seahorse XF24 demonstrated that the period during respiration when ATP is produced was down-regulated by approximately 50% in both BaF3/ITD-R and MV4-11-R cells when compared to BaF3/ITD and MV4-11 cells (Fig. 3D). However, we observed an approximately 15% decrease in total ATP levels in both the resistant cell lines when compared to the parental cell lines (Fig. 3D), indicating that a compensatory pathway is maintaining energy supply when mitochondrial oxidative phosphorylation is compromised.

Upregulation of glycolytic activity in sorafenib-resistant cells

It is known that cells generate ATP through glycolysis and mitochondrial oxidative phosphorylation. Our findings showing a dysfunction of the mitochondrial respiratory chain prompted us to examine the gene set profiling glycolytic pathways. As the microarray analysis illustrated in Fig. 4A, a majority of genes encoding glycolytic enzymes was up-regulated in MV4-11-R cells. Real-time PCR and western blotting analysis (Fig. 4B and C) further confirmed a significant increase in the expression of glycolytic genes and proteins, including hexokinase 2 (HK2), the enzyme that catalyzes the first and rate-limiting reaction during glycolysis, pyruvate kinase 2 (PKM2), the enzyme that catalyzes their reversible transfer of a phosphoryl group to yield ATP and pyruvate, and pyruvate dehydrogenase kinase 1 (PDK1), the enzyme that inactivates pyruvate dehydrogenase and prevents pyruvate from entering the TCA cycle in the mitochondria. We also tested the enzymatic activity of glyceraldehyde-3-phosphate dehydrogenase (GAPDH), a classical glycolytic enzyme commonly termed a 'housekeeping gene'. The enzyme kinetics of MV4-11 and MV4-11-R cells were monitored for 20 min, and Fig. 4D demonstrated that GAPDH activity in MV4-11-R cells was up-regulated by approximately 30% when compared to MV4-11cells.

It is known that during glycolysis, glucose is converted to pyruvate, resulting in a net production and extrusion of protons into the extracellular medium. We demonstrated a 50% increase in glucose uptake and a 2-fold increase in lactate production in MV4-11-R cells when compared to the parental cells (Fig. 4E). Extracellular acidification rate (ECAR), which reflects lactate production, was further examined by Seahorse XF Glycolysis Stress Test. Cells were

Please cite this article in press as: Amin Huang, et al., Metabolic alterations and drug sensitivity of tyrosine kinase inhibitor resistant leukemia cells with a FLT3/ITD mutation, Cancer Letters (2016), doi: 10.1016/j.canlet.2016.04.040

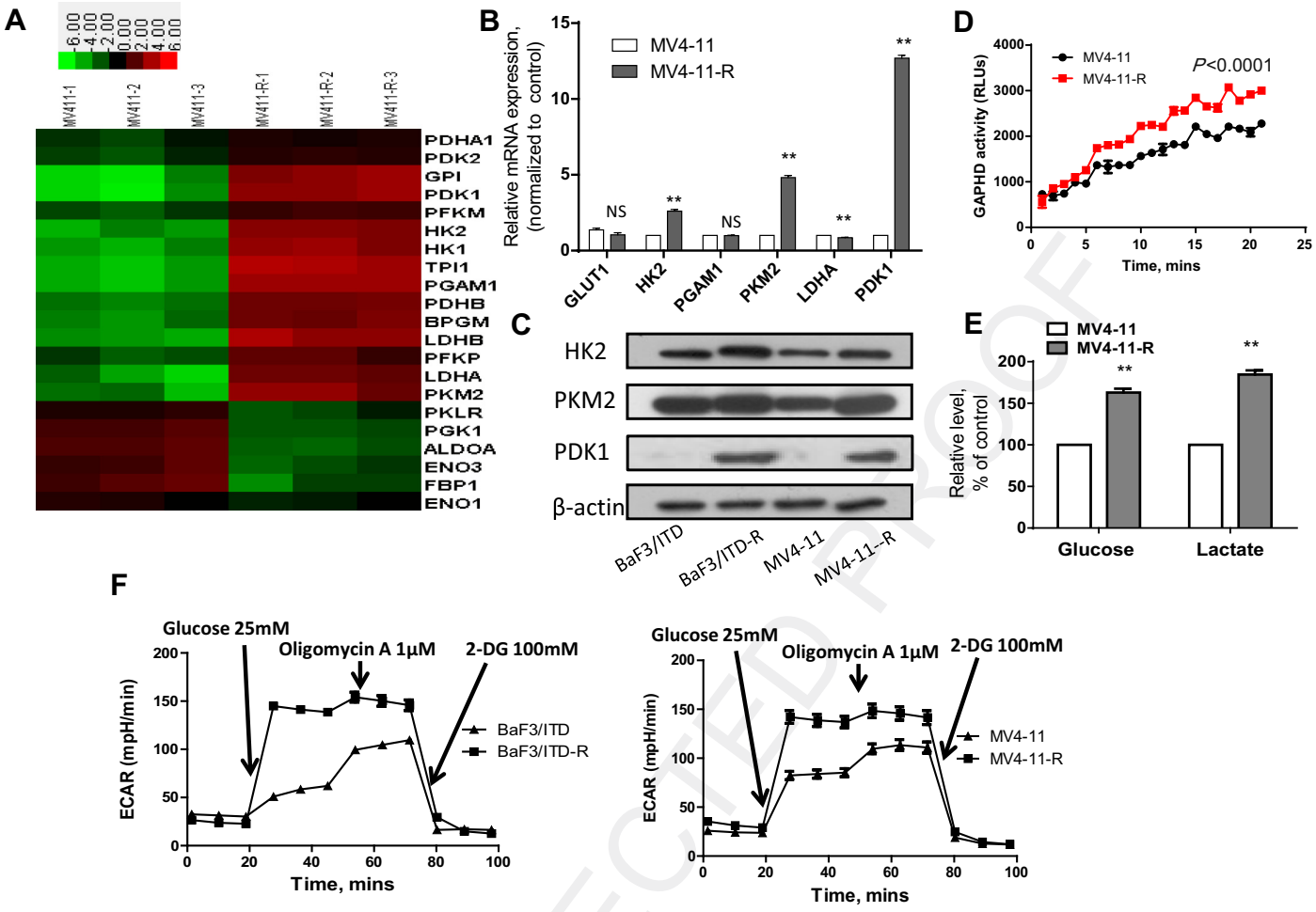

Fig. 4. Upregulation of glycolytic activity in sorafenib-resistant cells. (A) Comparative gene analysis of glycolytic enzymes that are significantly changed in MV4-11-R cells as determined by mRNA microarray. Red signal indicates higher expression and green signal indicates lower expression relative to the mean expression levels within the group. (B) Comparison of mRNA expression of glycolytic enzymes in MV4-11 and MV4-11-R cells by real-time PCR analysis. Bars, means ± SEM. **$p < 0.01$, $n = 3$. NS, non-significant. (C) Immunoblotting analysis of the major glycolytic enzymes HK2, PKM2 and PDK1 in BaF3/ITD, BaF3/ITD-R, MV4-11 and MV4-11-R cells. (D) A GAPDH enzyme activity assay in MV4-11 and MV4-11-R was performed as described in the Materials and methods section. The results were statistically significant ($p < 0.0001$). (E) Relative levels (% of control) of glucose uptake and lactate production in MV4-11-R cells compared with the parental MV4-11. Bars, means ± SEM. **$p < 0.01$, $n = 3$. (F) Pharmacological profile of extra cellular acidification rate (ECAR) was monitored with a Seahorse XF24 analyzer for 100 min. The metabolic inhibitors glucose, oligomycin A and 2-DG were injected sequentially at different time points as indicated. Left panel: Murine cells BaF3/ITD and BaF3/ITD-R. Right panel: Human cells MV4-11 and MV4-11-R. (For interpretation of the references to color in this figure legend, the reader is referred to the web version of this article.)

incubated in a glucose-free medium for 45 min before first injection of a saturating concentration of glucose (25 mM). As shown in Fig. 4F, addition of glucose induced a rapid increase in ECAR by both BaF3/ITD-R and MV4-11-R cells when compared to the parental cells. The second injection, oligomycin (1 μM), an ATP synthase inhibitor used to suppress mitochondrial ATP production and shift energy production to glycolysis, further increased lactate production and revealed a higher maximum glycolytic capacity in both sorafenib-resistant cell lines. The final injection, 2-deoxy-glucose (2-DG, 100 mM), was used to inhibit glycolysis through competitive binding to hexokinase and caused a rapid decrease in ECAR, confirming that the lactate production observed during the assay was due to glycolysis.

Effective killing of sorafenib-resistant cells by inhibition of glycolysis

The metabolic alterations observed in sorafenib-resistant cells and upregulation of major glycolytic enzymes prompted us to test if we could overcome drug resistance using glycolytic inhibitors. 3-BrOP is a known inhibitor of both hexokinase and GAPDH and has a potent inhibitory effect on glycolysis [17,28]. 2-DG is phosphorylated by hexokinase to generate 2-deoxyglucose-phosphate, which accumulates in cells and presumably inhibits hexokinase by a product-mediated inhibition [29,30]. Dichloroacetate (DCA) constrains the glycolytic pathway by inhibiting pyruvate dehydrogenase kinase (PDK) [31]. 3-BrOP, 2-DG and DCA were tested for cytotoxicity against the parental and resistant cell lines. As the MTS assay shown in Fig. 5A–C, BaF3/ITD-R and MV4-11-R cells showed lower IC_{50} values (1.9- to 7.6-fold) of 3-BrOP and 2-DG when compared to the parental BaF3/ITD and MV4-11 cells. Both BaF3/ITD-R (21 vs. 19 mM) and MV4-11-R (20 vs. 19 mM) appeared to be equally sensitive to DCA when compared to the parental cells. It has been reported that the highly glycolytic phenotype of cancer cells is supported by an over-expressed, outer mitochondrial membrane–bound hexokinase; the mitochondrial hexokinase plays a major role in preventing apoptosis by regulating the access of mitochondrial permeability transition pore complex (MPTP) to Bcl-2 family [32]. Here we demonstrated upregulation of HK2 in whole cell lysates

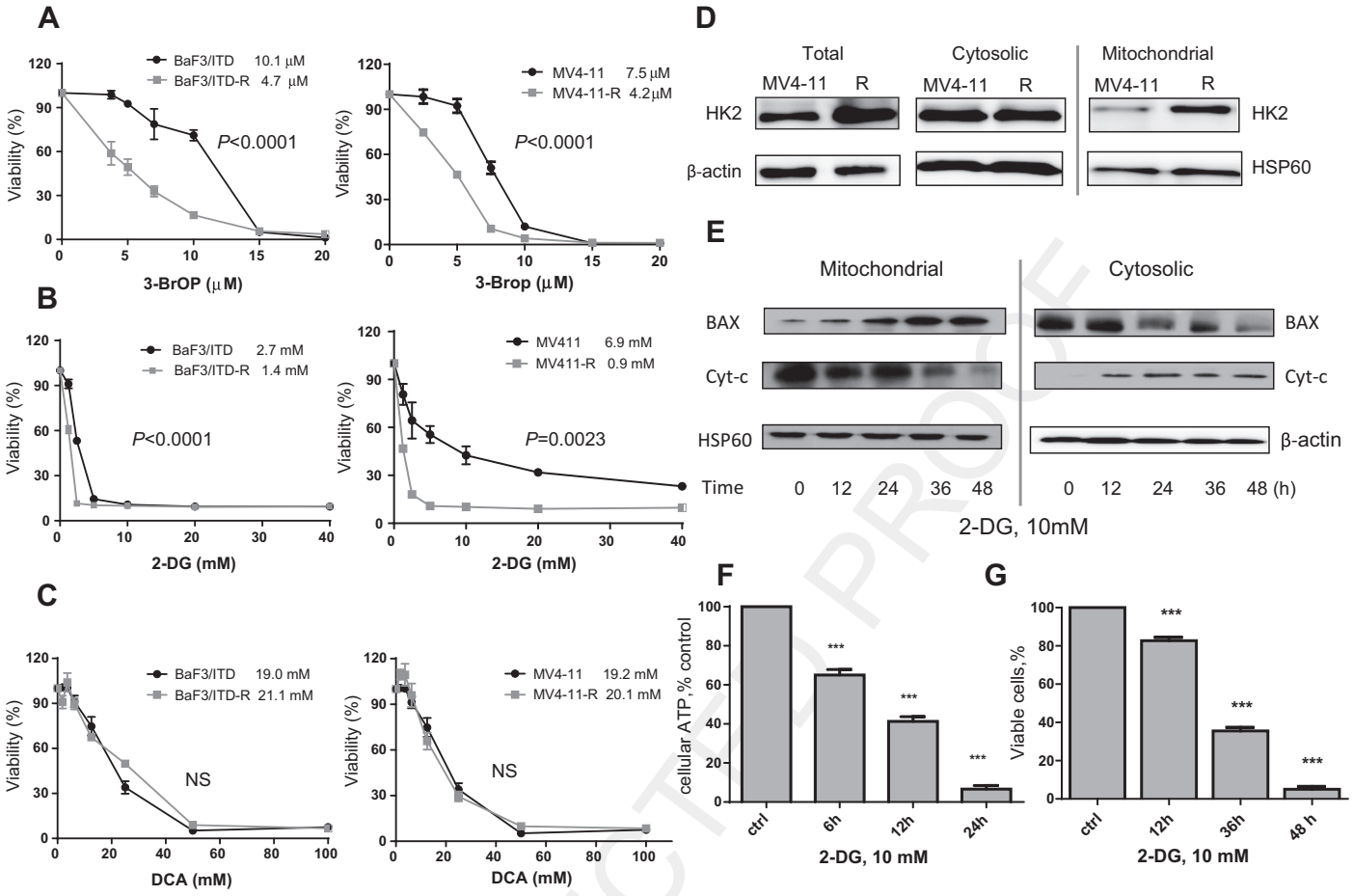

Fig. 5. Sorafenib-resistant cells are sensitive to glycolytic inhibitors. (A–C) BaF3/ITD, BaF3/ITD-R, MV4-11 and MV4-11-R cells were treated with various concentrations of glycolytic inhibitors including 3-BROP, 2-DG and DCA for 72 h and subjected to MTS assay. IC_{50} values of these compounds in each cell line and statistical significance levels were shown above the curves. NS, non-significant. (D) Western blotting analysis of HK2 expression in total cell lysates, cytosolic and mitochondrial fraction of MV4-11 and MV4-11-R cells. HSP60 was used as loading control for mitochondrial proteins. (E) MV4-11-R cells were treated with 10 mM 2-DG for the indicated times, and mitochondrial and cytosolic fractions were isolated and subjected for western blotting analysis for BAX and cytochrome c (Cyt-c). HSP60 was used as loading control for mitochondrial proteins. (F) MV4-11-R cells were treated with 10 mM 2-DG for different time points and subjected to analysis of cellular ATP levels as described in the Materials and methods section. (G) Time-dependent killing of MV4-11-R cells by treatment of 10 mM 2-DG as measured by annexin-V/PI assay. Bars, means ± SEM. ***$p < 0.001$, $n = 3$.

of MV4-11-R cells when compared to MV4-11cells, and we further observed a significant increase in HK2 in the mitochondrial fraction (Fig. 5D). In contrast, the MV4-11-R cells did not show a detectable increase inHK2 in the cytosolic fraction when compared to the parental cells. Our findings suggest that mitochondrial HK2 may be associated with escape from cell death in sorafenib-resistant leukemia cells. We then tested the effect of an HK2 inhibitor on the pro-apoptotic functions of resistant cells. Western blot analysis showed that incubation of MV4-11-R cells with 10 mM 2-DG caused a time-dependent increase in BAX protein expression in the mitochondrial fraction and also a decrease in BAX protein in the cytosolic fraction, suggesting BAX translocation into the mitochondria (Fig. 5E). As a result, translocation of BAX caused a change of mitochondrial membrane permeability and subsequent release of cytochrome c from the mitochondria in to the cytosol (Fig. 5E). In addition, 2-DG caused a time-dependent depletion of cellular ATP in MV4-11-R cells as early as 6 h and a nearly complete depletion at 24 h; significant cell death was not observed until 12 h and massive cell death occurred approximately at 48 h, validating the logical approach to inhibit glycolysis, a process that compensates for mitochondrial dysfunction and effectively kills sorafenib-resistant cells.

Discussion

Dependence of cancer cells on glycolysis for generation of ATP has long been recognized as the Warburg effect and is considered one of the most fundamental metabolic alterations during malignant transformation. However, the association between metabolic alterations and drug resistance and the therapeutic implications of altering metabolism remained to be investigated. Here, we established the murine (BaF3/ITD-R) and human (MV4-11-R) sorafenib-resistant cell lines carrying the FLT3/ITD mutation, and we showed that these resistant cell lines exhibited cross-resistance to both type I (PKC412) and type II (sorafenib, MLN518) tyrosine kinase inhibitors.

mRNA microarray and Ingenuity Pathway Analysis (IPA) of MV4-11 and MV11-R cells revealed that mitochondrial dysfunction was identified as the highest-ranked molecular and cellular function in the differential gene sets from MV4-11-R cells. Further biochemical measurements of oxygen consumption, glucose uptake and lactate production identified a metabolic alteration in both murine and human sorafenib-resistant cell lines, including a substantial decrease in mitochondria-derived ATP produced and a significant increase in glycolytic activity to maintain sufficient ATP production. These metabolic changes seem to be associated with

Please cite this article in press as: Amin Huang, et al., Metabolic alterations and drug sensitivity of tyrosine kinase inhibitor resistant leukemia cells with a FLT3/ITD mutation, Cancer Letters (2016), doi: 10.1016/j.canlet.2016.04.040

deregulation of the mitochondrial electron transport chain (ECT), as we observed a substantial decrease in the expression of the ECT complex I, which is the entry point of electrons into the oxidative phosphorylation/ATP-generating system [25]. The upregulation of major glycolytic enzymes, including HK2, PKM2 and PDK1, also indicates that the resistant cells have a higher glycolytic flux.

Thus, the dysfunctional mitochondria and activated glycolysis observed in the FLT3/ITD-positive sorafenib-resistant cells appeared to be consistent with the Warburg effect, which has long been recognized as the most important hallmark of oncogenesis [13]. In the current study, dependence on the glycolytic pathway to generate ATP suggests that sorafenib-resistant cells might be vulnerable to glycolytic inhibition. High levels of glycolytic enzymes, including HK2 and PDK1, and increased activity of GAPDH prompted us to investigate the effects of various glycolytic inhibitors. Our previous studies demonstrated 3-BrOP as an effective inhibitor of both HK2 and GAPDH [17,28]. 2-DG mainly inhibited glycolysis at the rate-limiting step of glucose phosphorylation by hexokinase [28]. Here, sorafenib-resistant cells showed an increased sensitivity to both 3-BrOP and 2-DG compared with the parental cells. In addition, a key point linking glycolysis with the mitochondrial tricarboxylic acid cycle (TCA cycle) for cellular respiration is the oxidative decarboxylation of pyruvate to acetyl-CoA, catalyzed by pyruvate dehydrogenase (PDH) [33]. Pyruvate dehydrogenase kinases1 (PDK1) has been reported as a key regulator of the Warburg effect by inhibiting PDH and shuttling pyruvate away from the TCA cycle [34]. In addition to exhibiting high levels of PDK1, sorafenib-resistant cells remained sensitive to dichloroacetate (DCA), a known small molecule inhibitor of PDK activity.

It is noteworthy that a predominant fraction of HK2 binds to voltage-dependent anion channel (VDAC) found on the outer mitochondrial membrane, and VDAC plays an important role in regulating mitochondrial permeability and the release of the apoptotic factor cytochrome c [32,35]. We speculated that the upregulation of HK2 in sorafenib-resistant cells may not only contribute to metabolic alterations but also set a higher threshold for mitochondria outer membrane permeability to prevent the induction of apoptosis. Indeed, we showed that the increase of HK2 was mainly found in the mitochondrial fraction of sorafenib-resistant cells. Hexokinase inhibitor2-DG caused a decrease in ATP generation, translocation of pro-apoptotic family member BAX to mitochondria and subsequent release of cytochrome c. Notably, Akt has been shown to promote binding of HK2 to VDAC, leading to inhibition of apoptosis [36,37]. In agreement with a previous work, our study showed activation of the AKT pathway in sorafenib-resistant cells, although phosphorylated FLT3 remained inhibited. These findings agree with a previous study on sorafenib-resistant cells harboring an acquired point mutation in the FLT3 gene, which showed that the inhibition of phosphorylated FLT3 was not sufficient to inhibit its downstream effector, including AKT [38]. Moreover, when compared to the parental cells, sorafenib-resistant cells showed significantly greater sensitivity to hexokinase inhibitors, including 3-BrOP and 2-DG, rather than the PDK inhibitor DCA. These findings may indicate an increased dependence on hexokinase for energy supplies and vulnerability to hexokinase inhibitors in sorafenib-resistant cells. As such, our study suggests that glycolytic enzymes such as HK2 might be the preferred therapeutic target to overcome sorafenib resistance regardless of the mutation status of the FLT3 gene.

It is interesting to note that the sorafenib-resistant cells exhibited a longer doubling time, which is consistent with G2 cell cycle arrest and delay in entry into mitosis. Although we did not test the mechanistic link of molecular features to cell cycle arrest in the current study, we did observe a substantial increase of oxidative stress in the resistant cells (data not shown), which might lead to DNA damage and subsequent induction of G2 arrest.

In summary, our study revealed a metabolic signature of sorafenib-resistant cells and indicated an increase of glycolytic activity, including upregulation of major glycolytic enzymes. These enzymes may be markers for resistance to FLT3 and glycolytic inhibitors and warrant further investigation as alternative therapeutic agents for FLT3/ITD leukemia.

Funding

This study was supported by research grants from Guangdong Natural Science Foundation (No. 2014A030313037), National Basic Research Program of China (973 program, No. 2013CB910304) and Guangzhou Technology Program (No. 201504010038 and No. 201508020250).

Acknowledgements

We gratefully thank Dr. Donald Small for providing the BaF3/ITD cell line.

Conflict of interest

The authors declare that they have no competing interests.

Appendix: Supplementary material

Supplementary data to this article can be found online at doi:10.1016/j.canlet.2016.04.040.

References

[1] C. Thiede, C. Steudel, B. Mohr, M. Schaich, U. Schakel, U. Platzbecker, et al., Analysis of FLT3-activating mutations in 979 patients with acute myelogenous leukemia: association with FAB subtypes and identification of subgroups with poor prognosis, Blood 99 (2002) 4326–4335.
[2] S.P. Whitman, K.J. Archer, L. Feng, C. Baldus, B. Becknell, B.D. Carlson, et al., Absence of the wild-type allele predicts poor prognosis in adult de novo acute myeloid leukemia with normal cytogenetics and the internal tandem duplication of FLT3: a cancer and leukemia group B study, Cancer Res. 61 (2001) 7233–7239.
[3] H. Konig, M. Levis, Targeting FLT3 to treat leukemia, Expert Opin. Ther. Targets 19 (2015) 37–54.
[4] N. Daver, J. Cortes, F. Ravandi, K.P. Patel, J.A. Burger, M. Konopleva, et al., Secondary mutations as mediators of resistance to targeted therapy in leukemia, Blood 125 (2015) 3236–3245.
[5] S.H. Chu, D. Small, Mechanisms of resistance to FLT3 inhibitors, Drug Resist. Updat. 12 (2009) 8–16.
[6] C.H. Man, T.K. Fung, C. Ho, H.H. Han, H.C. Chow, A.C. Ma, et al., Sorafenib treatment of FLT3-ITD(+) acute myeloid leukemia: favorable initial outcome and mechanisms of subsequent nonresponsiveness associated with the emergence of a D835 mutation, Blood 119 (2012) 5133–5143.
[7] C.C. Smith, Q. Wang, C.S. Chin, S. Salerno, L.E. Damon, M.J. Levis, et al., Validation of ITD mutations in FLT3 as a therapeutic target in human acute myeloid leukaemia, Nature 485 (2012) 260–263.
[8] A.B. Williams, B. Nguyen, L. Li, P. Brown, M. Levis, D. Leahy, et al., Mutations of FLT3/ITD confer resistance to multiple tyrosine kinase inhibitors, Leukemia 27 (2013) 48–55.
[9] E.V. Barry, J.J. Clark, J. Cools, J. Roesel, D.G. Gilliland, Uniform sensitivity of FLT3 activation loop mutants to the tyrosine kinase inhibitor midostaurin, Blood 110 (2007) 4476–4479.
[10] E. Weisberg, M. Sattler, A. Ray, J.D. Griffin, Drug resistance in mutant FLT3-positive AML, Oncogene 29 (2010) 5120–5134.
[11] O. Piloto, M. Wright, P. Brown, K.T. Kim, M. Levis, D. Small, Prolonged exposure to FLT3 inhibitors leads to resistance via activation of parallel signaling pathways, Blood 109 (2007) 1643–1652.
[12] E. Siendones, N. Barbarroja, L.A. Torres, P. Buendia, F. Velasco, G. Dorado, et al., Inhibition of Flt3-activating mutations does not prevent constitutive activation of ERK/Akt/STAT pathways in some AML cells: a possible cause for the limited effectiveness of monotherapy with small-molecule inhibitors, Hematol. Oncol. 25 (2007) 30–37.
[13] D. Hanahan, R.A. Weinberg, Hallmarks of cancer: the next generation, Cell 144 (2011) 646–674.
[14] J.F. Geschwind, C.S. Georgiades, Y.H. Ko, P.L. Pedersen, Recently elucidated energy catabolism pathways provide opportunities for novel treatments in hepatocellular carcinoma, Expert Rev. Anticancer Ther. 4 (2004) 449–457.

[15] J.C. Maher, A. Krishan, T.J. Lampidis, Greater cell cycle inhibition and cytotoxicity induced by 2-deoxy-D-glucose in tumor cells treated under hypoxic vs aerobic conditions, Cancer Chemother. Pharmacol. 53 (2004) 116–122.
[16] S. Yuan, F. Wang, G. Chen, H. Zhang, L. Feng, L. Wang, et al., Effective elimination of cancer stem cells by a novel drug combination strategy, Stem Cells 31 (2013) 23–34.
[17] Z. Tang, S. Yuan, Y. Hu, H. Zhang, W. Wu, Z. Zeng, et al., Over-expression of GAPDH in human colorectal carcinoma as a preferred target of 3-bromopyruvate propyl ester, J. Bioenerg. Biomembr. 44 (2012) 117–125.
[18] Y. Zhou, Y. Zhou, T. Shingu, L. Feng, Z. Chen, M. Ogasawara, et al., Metabolic alterations in highly tumorigenic glioblastoma cells: preference for hypoxia and high dependency on glycolysis, J. Biol. Chem. 286 (2011) 32843–32853.
[19] K.F. Tse, J. Allebach, M. Levis, B.D. Smith, F.D. Bohmer, D. Small, Inhibition of the transforming activity of FLT3 internal tandem duplication mutants from AML patients by a tyrosine kinase inhibitor, Leukemia 16 (2002) 2027–2036.
[20] R.H. Xu, H. Pelicano, H. Zhang, F.J. Giles, M.J. Keating, P. Huang, Synergistic effect of targeting mTOR by rapamycin and depleting ATP by inhibition of glycolysis in lymphoma and leukemia cells, Leukemia 19 (2005) 2153–2158.
[21] Y. Hu, W. Lu, G. Chen, H. Zhang, Y. Jia, Y. Wei, et al., Overcoming resistance to histone deacetylase inhibitors in human leukemia with the redox modulating compound beta-phenylethyl isothiocyanate, Blood 116 (2010) 2732–2741.
[22] Y. Hu, W. Lu, G. Chen, P. Wang, Z. Chen, Y. Zhou, et al., K-ras(G12 V) transformation leads to mitochondrial dysfunction and a metabolic switch from oxidative phosphorylation to glycolysis, Cell Res. 22 (2012) 399–412.
[23] R.M. Stone, D.J. DeAngelo, V. Klimek, I. Galinsky, E. Estey, S.D. Nimer, et al., Patients with acute myeloid leukemia and an activating mutation in FLT3 respond to a small-molecule FLT3 tyrosine kinase inhibitor, PKC412, Blood 105 (2005) 54–60.
[24] D.J. DeAngelo, R.M. Stone, M.L. Heaney, S.D. Nimer, R.L. Paquette, R.B. Klisovic, et al., Phase 1 clinical results with tandutinib (MLN518), a novel FLT3 antagonist, in patients with acute myelogenous leukemia or high-risk myelodysplastic syndrome: safety, pharmacokinetics, and pharmacodynamics, Blood 108 (2006) 3674–3681.
[25] D.D. Newmeyer, S. Ferguson-Miller, Mitochondria: releasing power for life and unleashing the machineries of death, Cell 112 (2003) 481–490.
[26] M. Wu, A. Neilson, A.L. Swift, R. Moran, J. Tamagnine, D. Parslow, et al., Multiparameter metabolic analysis reveals a close link between attenuated mitochondrial bioenergetic function and enhanced glycolysis dependency in human tumor cells, Am. J. Physiol. Cell Physiol. 292 (2007) C125–C136.
[27] W. Qian, B. Van Houten, Alterations in bioenergetics due to changes in mitochondrial DNA copy number, Methods 51 (2010) 452–457.
[28] R.H. Xu, H. Pelicano, Y. Zhou, J.S. Carew, L. Feng, K.N. Bhalla, et al., Inhibition of glycolysis in cancer cells: a novel strategy to overcome drug resistance associated with mitochondrial respiratory defect and hypoxia, Cancer Res. 65 (2005) 613–621.
[29] H. Pelicano, D.S. Martin, R.H. Xu, P. Huang, Glycolysis inhibition for anticancer treatment, Oncogene 25 (2006) 4633–4646.
[30] Z. Chen, W. Lu, C. Garcia-Prieto, P. Huang, The Warburg effect and its cancer therapeutic implications, J. Bioenerg. Biomembr. 39 (2007) 267–274.
[31] P.W. Stacpoole, The pharmacology of dichloroacetate, Metabolism 38 (1989) 1124–1144.
[32] S.P. Mathupala, Y.H. Ko, P.L. Pedersen, Hexokinase II: cancer's double-edged sword acting as both facilitator and gatekeeper of malignancy when bound to mitochondria, Oncogene 25 (2006) 4777–4786.
[33] G.J. Sale, P.J. Randle, Analysis of site occupancies in [32P]phosphorylated pyruvate dehydrogenase complexes by aspartyl-prolyl cleavage of tryptic phosphopeptides, Eur. J. Biochem. 120 (1981) 535–540.
[34] J.W. Kim, I. Tchernyshyov, G.L. Semenza, C.V. Dang, HIF-1-mediated expression of pyruvate dehydrogenase kinase: a metabolic switch required for cellular adaptation to hypoxia, Cell Metab. 3 (2006) 177–185.
[35] J.E. Wilson, Isozymes of mammalian hexokinase: structure, subcellular localization and metabolic function, J. Exp. Biol. 206 (2003) 2049–2057.
[36] K. Gottlob, N. Majewski, S. Kennedy, E. Kandel, R.B. Robey, N. Hay, Inhibition of early apoptotic events by Akt/PKB is dependent on the first committed step of glycolysis and mitochondrial hexokinase, Genes Dev. 15 (2001) 1406–1418.
[37] J.M. Bryson, P.E. Coy, K. Gottlob, N. Hay, R.B. Robey, Increased hexokinase activity, of either ectopic or endogenous origin, protects renal epithelial cells against acute oxidant-induced cell death, J. Biol. Chem. 277 (2002) 11392–11400.
[38] W. Zhang, C. Gao, M. Konopleva, Y. Chen, R.O. Jacamo, G. Borthakur, et al., Reversal of acquired drug resistance in FLT3-mutated acute myeloid leukemia cells via distinct drug combination strategies, Clin. Cancer Res. 20 (2014) 2363–2374.

Please cite this article in press as: Amin Huang, et al., Metabolic alterations and drug sensitivity of tyrosine kinase inhibitor resistant leukemia cells with a FLT3/ITD mutation, Cancer Letters (2016), doi: 10.1016/j.canlet.2016.04.040